Hindawi Publishing Corporation
Journal of Nanomaterials
Volume 2014, Article ID 284634, 7 pages
http://dx.doi.org/10.1155/2014/284634

Research Article

Investigation of the Microstructural and Thermoelectric Properties of the $(GeTe)_{0.95}(Bi_2Te_3)_{0.05}$ Composition for Thermoelectric Power Generation Applications

Lior Weintraub,[1] Joseph Davidow,[2] Jonathan Tunbridge,[3] Richard Dixon,[3] Michael John Reece,[4] Huanpo Ning,[4] Iñigo Agote,[5] and Yaniv Gelbstein[1,2]

[1] *Unit of Energy Engineering, Ben-Gurion University of the Negev, Beer-Sheva, Israel*
[2] *Department of Materials Engineering, Ben-Gurion University of the Negev, Beer-Sheva, Israel*
[3] *Intrinsiq Materials Ltd., Cody Technology Park, Farnborough GU14OLX, UK*
[4] *School of Engineering and Materials Science, Queen Mary, University of London, Mile End Road, London E1 4NS, UK*
[5] *TECNALIA Research & Innovation, Mikeletegi Pasealekua, 2 20009 San Sebastian, Spain*

Correspondence should be addressed to Yaniv Gelbstein; yanivge@bgu.ac.il

Received 12 June 2013; Accepted 5 December 2013; Published 19 January 2014

Academic Editor: Won-Seon Seo

In the frame of the current research, the *p*-type Bi_2Te_3 doped $(GeTe)_{0.95}(Bi_2Te_3)_{0.05}$ alloy composed of hot pressed consolidated submicron structured powder was investigated. The influence of the process parameters (i.e., powder particles size and hot pressing conditions) on both reduction of the lattice thermal conductivity and electronic optimization is described in detail. Very high maximal *ZT* values of up to ~1.6 were obtained and correlated to the microstructural characteristics. Based on the various involved mechanisms, a potential route for further enhancement of the *ZT* values of the investigated composition is proposed.

1. Introduction

Thermoelectrics as a direct energy conversion method between heat and electricity is mainly used for electrical power generation and cooling applications. Germanium telluride based alloys are known as appropriate candidates for *p*-type legs in thermoelectric applications for the 50–500°C temperature range, exhibiting high dimensionless thermoelectric figure of merit ($ZT = (\alpha^2 T)/(\rho\kappa)$, where α is the Seebeck coefficient, ρ is the electrical resistivity, κ is thermal conductivity, and T is absolute temperature) values. GeTe based compounds are characterized by a continuous phase transition from a low temperature rhombohedral to a high temperature cubic rock salt structure that takes place at 427°C in pure GeTe [1].

Germanium telluride based alloys are characterized by a large deviation from stoichiometry toward tellurium rich compositions. The main nonstoichiometric defects are doubly ionized metal vacancies. As a result of this deviation from stoichiometry, GeTe always exhibits *p*-type conductivity (p ~10^{20}–10^{21} cm^{-3}) [2]. To reduce the hole concentration, in order to obtain optimal thermoelectric properties, it is necessary to dope GeTe with donor type electroactive impurities. Bi_2Te_3 [3] and PbTe [4] act as donors while dissolved in GeTe. A mechanism of doping GeTe by Bi_2Te_3 has been put forward by Gelbstein et al. [2], according to which the latter is implanted into the GeTe lattice in the form of complexes consisting of a single electroneutral cation vacancy per each Bi_2Te_3 molecule implanted. The introduction of Bi_2Te_3 into the GeTe lattice changes the cation-anion ratio and the vacancy formation is due to the requirement for charge equilibrium. The reduction of the hole concentration in GeTe after introducing Bi_2Te_3 is associated with the filling of the cation vacancies by germanium atoms present in GeTe as a second phase. High thermoelectric performance was recently reported by PbTe alloying of GeTe

for obtaining quasi-binary $(GeTe)_x(PbTe)_{1-x}$ alloys that can be designed for achieving improved electronic properties and lower lattice thermal conductivities, as compared to PbTe and GeTe, separately, via phase separation reactions [5].

The present communication is concerned with the possibility of increasing the thermoelectric figure of merit of *p*-type Bi_2Te_3 doped $(GeTe)_{0.95}(Bi_2Te_3)_{0.05}$ alloy, by optimizing various powder metallurgy parameters (i.e., powder milling and hot pressing conditions) for obtaining both submicrofeatures, resulting in reduced lattice thermal conductivity values, and optimal electronic doping. The combined effects on the resultant *ZT* values are discussed in detail.

2. Experimental

$(GeTe)_{0.95}(Bi_2Te_3)_{0.05}$ was prepared by sealing the source materials (purity of 5N) at appropriate concentrations in a quartz ampoule under a vacuum of 10^{-5} Torr and melting in a rocking furnace at 850°C for 1 hour followed by water quenching. Various milling conditions of the cast ingot to a maximal powder particle size of 50 and 250 μm, using agate mortar and pestle, and to smaller sized powder, using energetic ball milling (Fritsch-Pulverisette 7) at 700 RPM following 10 and 20 cycles of 10 minutes each, were applied. The 50 and 250 μm maximal sieved powder were subsequently hot pressed (HPW5 Hot Press FCT Systeme GmbH) under a mechanical pressure of 35 MPa at 450°C and 650°C for 30 minutes, resulting in high density values of ~95 and ~97% of the theoretical density, respectively.

Seebeck coefficient (α) and the electrical resistivity (ρ) measurements were carried out in a self-constructed apparatus under an argon atmosphere up to ~450°C at a heating rate of 3°C/min. For the Seebeck coefficient measurements, an auxiliary heater was used to maintain a temperature difference of 10°C between the extremities of the samples. Electrical resistivity was measured by the "four-probe" method using an alternating power source of 1 V/50 Hz.

The thermal conductivity (κ) was determined as a function of temperature from room temperature to 500°C using the flash diffusivity method (LFA 457, Netzsch). The front face of a disc-shaped sample (ϕ = 12 mm, thickness ≈ 1-2 mm) is irradiated by a short laser burst, and the resulting rear face temperature is recorded and analyzed. Thermal conductivity values were calculated using the equation $\kappa = \gamma \cdot C_P \cdot \delta$, where γ is the thermal diffusivity, C_P is the specific heat (measured using differential scanning calorimetry, STA 449, Netzsch), and δ is the bulk density of the sample (calculated from the sample's geometry and its mass). The room temperature C_P value for all of the investigated synthesis conditions was found to be equal to 0.23 ± 0.01 J/grK.

The structural characteristics of the various investigated powder conditions were analyzed by high resolution scanning electron microscopy (Jeol-7400F HRSEM), transmission electron microscopy (TEM-FEI TECNAI-G^2), and X-ray diffraction (Rigaku DMAX 2100 powder diffractometer). The mean size, *d*, of the apparent submicron crystalline domains was obtained by applying Scherrer equation, $d = (K\lambda)/(\omega \cos\theta)$, where λ represents the wavelength of the X-ray radiation, θ is the angle of the considered Bragg reflection, ω is the peaks width on a 2θ scale, and K is a constant close to unity, to the experimental X-Ray diffraction peaks.

3. Results and Discussion

3.1. Powder Structural Characteristics. The microstructure of the $(GeTe)_{0.95}(Bi_2Te_3)_{0.05}$ powder hand crushed and sieved to a maximal powder particle size of 50 μm is shown in Figures 1(a)–1(c).

It can be easily seen from these figures that the 50 μm powder exhibits large microscale agglomerates composed of less than 5 μm powder domains, Figures 1(a) and 1(b), which are composed of even finer particles of less than 300 nm particles, as was observed by TEM analysis (Figure 1(c)). A very similar microstructure was also observed for the powder obtained following hand crushing and sieving to a maximal powder particle size of 250 μm, indicating that the basic minimal powder particles are much smaller in size than the actually sieved microscale powder agglomerates for this specific composition. Following 700 RPM, 10 and 20 cycles of 10 minutes each, even finer particles than 100 nm were identified, as indicated in Figure 1(d). No finer details could be distinguished by the SEM for the 20-cycle ball milling compared to the 10 cycles' process.

Room temperature XRD analysis following the various applied synthesis conditions, including the high temperature melting (850°C), and hot pressing (450 and 650°C) conditions, obtained at higher temperatures than the rhombohedral to cubic phase transition (~430°C for pure GeTe), exhibited the typical low temperature rhombohedral structure, being as expected in agreement with the equilibrium phase diagram.

Typical XRD patterns of the 50 and 250 μm hand crushed and sieved powder and ball milled at 700 RPM for 10 and 20 cycles of 10 minutes each are shown in Figure 2. The figure illustrates a typical doublet, characteristic of the low temperature rhombohedral phase of GeTe, which exhibits broadened widths with increasing the applied mechanical forces during the milling process. For the larger agglomerate powder, hand crushed and sieved to 250 and 50 μm, relatively narrow peaks were observed, which were analyzed to correspond to average grain size of 40–60 nm, in agreement with the finest grains of less than 300 nm observed by TEM (Figure 1(c)). Increasing the applied mechanical forces during the 700 RPM energetic ball milling procedure resulted in much broadened peaks, corresponding to finer average grain sizes of 20–25 nm. Yet, due to the fact that these large peaks have broadening effect, evidenced in some amorphization of the originally synthesized crystalline GeTe phase, and therefore are expected to degrade the electronic transport properties of the investigated $(GeTe)_{0.95}(Bi_2Te_3)_{0.05}$ composition, it was decided to focus in the next stages of the research on investigation of the transport properties of the larger domains powder following 50 and 250 μm sieving, in which a higher level of crystallinity was preserved following the powdering action.

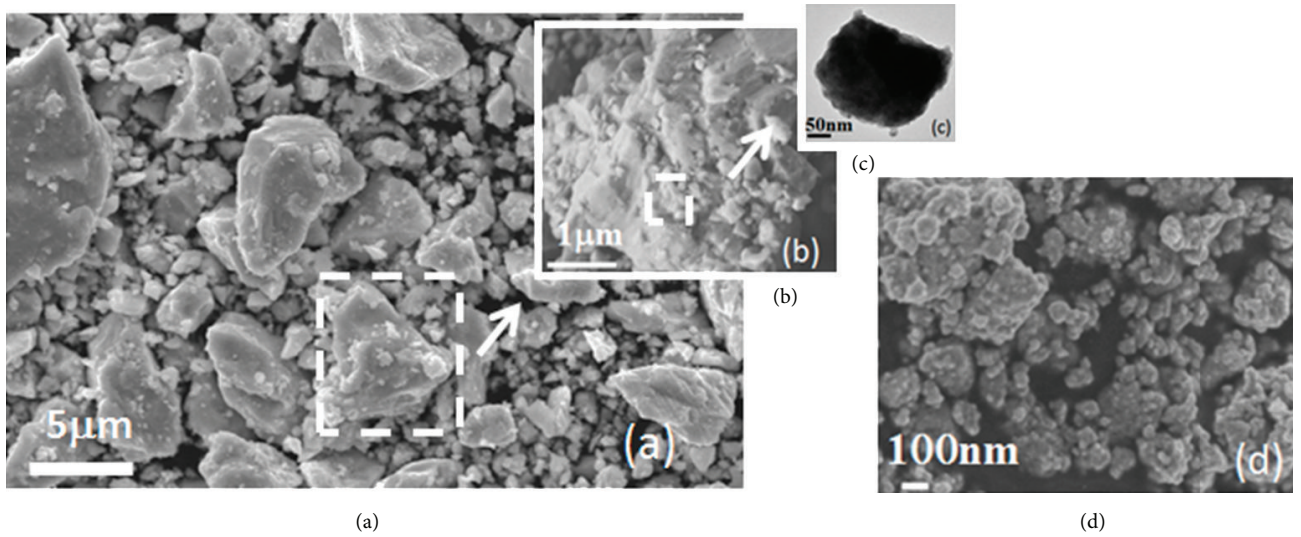

FIGURE 1: SEM (a), higher magnification SEM (b), TEM (c) images of $(GeTe)_{0.95}(Bi_2Te_3)_{0.05}$ hand crushed and sieved to maximal sized 50 μm powder, and HRSEM image of similar matrix composition following 10-cycles ball milling ball at 700 RPM/10 min (d).

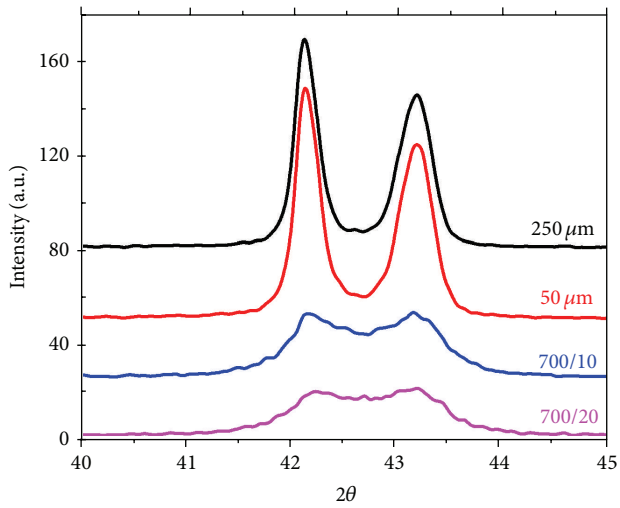

FIGURE 2: Powder XRD of $(GeTe)_{0.95}(Bi_2Te_3)_{0.05}$ following hand crushing for maximal powder particles size of 50 and 250 μm and following 10 and 20-cycle ball milling of 10 minutes at 700 RPM/10 min.

3.2. Transport Properties following Hot Pressing Consolidation. As was described above in the experimental section, two hot pressing temperatures of 450 and 650°C were investigated in the current research, yielding density values of ~95 and ~97% of the theoretical density, respectively. The 650°C (923 K) temperature, which is about 90% of the melting temperature, T_m, of pure GeTe compound (998 K [6]), was chosen due to the associated high diffusion rates of the involved elements at this temperature and the expected high homogeneity of the investigated composition. The lower hot pressing temperature (450°C) was chosen to be in the vicinity of the phase transition temperature (~430°C in pure GeTe, [6]) from a low temperature rhombohedral to a high temperature cubic structures. Both of these hot pressing temperatures, 650 and 450°C, were chosen as slightly lower than the melting temperature and the phase transition temperatures of pure GeTe, respectively, due to the understanding that the investigated $(GeTe)_{0.95}(Bi_2Te_3)_{0.05}$ matrix composition, obtained by 5% alloying with the low melting temperature Bi_2Te_3 phase (~585°C [7]), which is stable from low temperatures up to its melting, is expected to exhibit slightly lower melting temperature and lower phase transition temperatures, respectively, compared to pure GeTe.

The temperature dependencies of Seebeck coefficient, α, electrical resistivity, ρ, and thermal conductivity, κ, of the investigated $(GeTe)_{0.95}(Bi_2Te_3)_{0.05}$ composition following hand crushing and sieving to maximal powder agglomerates of 50 and 250 μm and hot pressing at 450 and 650°C are shown in Figures 3, 4, and 5, respectively.

Investigation of Figures 3 and 4 reveals that following 650°C hot pressing of both the 50 and 250 μm sieved powder agglomerates, nearly identical low temperature α and ρ values, with slightly higher values for the 50 μm sample, were observed, indicating similar associated carrier concentrations for both of the samples with slightly lower values for the 50 μm sample. This slightly lower overall carrier concentration for the 50 μm sample, in which slightly higher mechanical force was applied while crushing the sample to this smaller powder particles size sample, can be attributed to the strain induced compensation effect, in which as was already established for many telluride compounds (e.g. PbTe [8], $Pb_xSn_{1-x}Te$ [9], $Ge_xPb_{1-x}Te$ [10], and Bi_2Te_3 [11]), mechanical stresses can result in introduction of additional donor levels in the band gaps, and for the case of inherent p-type compositions, in reduction of the overall carrier concentration.

Although the general high similarity between the α and ρ values obtained following 650°C hot pressing for both of the investigated powder particle sizes, similar low temperature

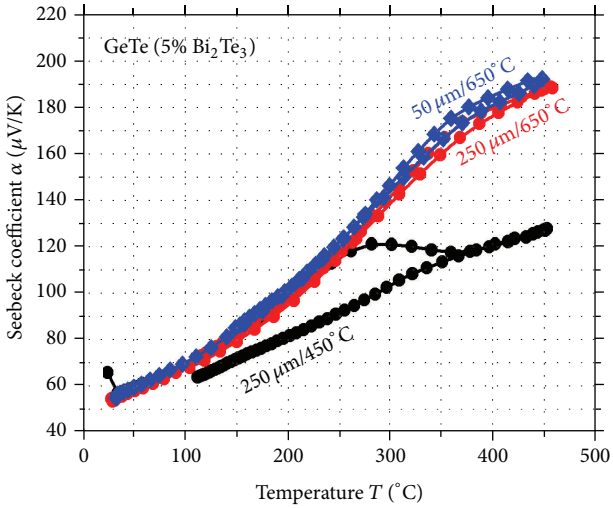

Figure 3: Temperature dependence of Seebeck coefficient, α, for $(GeTe)_{0.95}(Bi_2Te_3)_{0.05}$ following hand crushing for maximal powder particles size of 50 and 250 μm and hot pressing at 650°C (50 μm/650°C and 250 μm/650°C, resp.) and for 250 μm hot pressed powder at 450°C (250 μm/450°C).

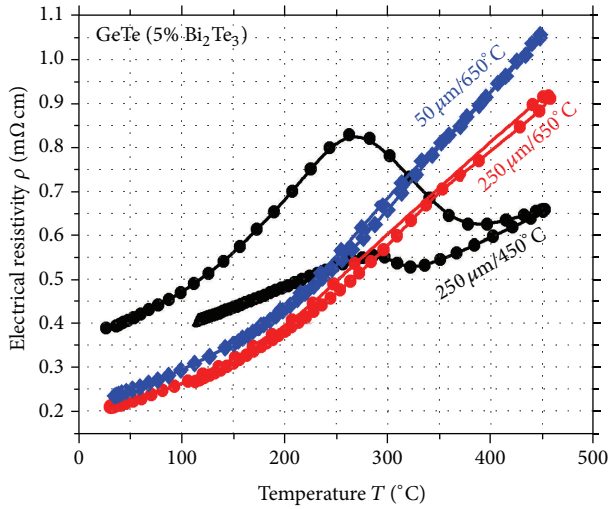

Figure 4: Temperature dependence of the electrical resistivity, ρ, for $(GeTe)_{0.95}(Bi_2Te_3)_{0.05}$ following hand crushing for maximal powder particles size of 50 and 250 μm and hot pressing at 650°C (50 μm/650°C and 250 μm/650°C, resp.) and for 250 μm hot pressed powder at 450°C (250 μm/450°C).

Seebeck coefficient values accompanied by much higher low temperature electrical resistivity values were obtained following hot pressing at 450°C of maximal 250 μm sieved powder particles, as shown in Figures 3 and 4. This evidence can be attributed to carrier concentration, p, values similar to those obtained following the 650°C hot pressing, as indicated by the similar α values, but lower carrier mobility, μ, values, as indicated by the higher ρ values ($\rho = (p \cdot e \cdot \mu)^{-1}$) which can result from a lower homogeneity state of this sample, which was hot pressed at much lower temperature than for the case

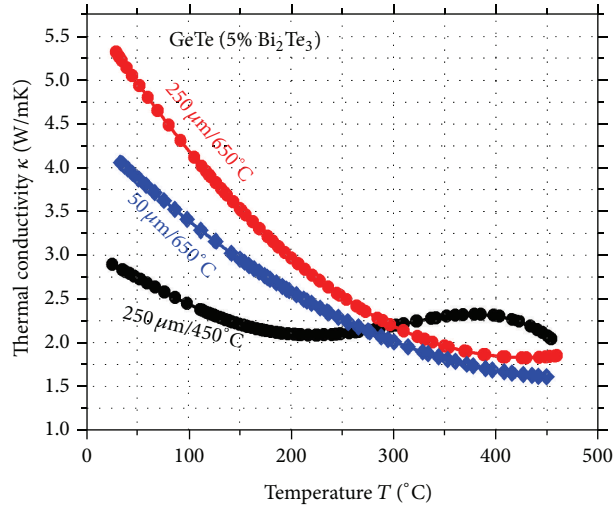

Figure 5: Temperature dependence of the thermal conductivity, κ, for $(GeTe)_{0.95}(Bi_2Te_3)_{0.05}$ following hand crushing for maximal powder particles size of 50 and 250 μm and hot pressing at 650°C (50 μm/650°C and 250 μm/650°C, resp.) and for 250 μm hot pressed powder at 450°C (250 μm/450°C).

of the 650°C hot pressing, and can be associated with lower diffusion rates of the involved elements.

Furthermore, both of the α and ρ temperature dependencies of the 450°C hot pressed sample were totally different from those obtained following the 650°C hot pressing procedures. Following the 450°C hot pressing conditions, a thermal hysteresis was observed between the heating and cooling cycles while measuring both α and ρ values, with the most pronounced differences in the 100–400°C temperature range. This abnormal α and ρ temperature dependent trend can result from the second order phase transition, associated with GeTe based compounds, as was previously reported for single crystal grown $Ge_xPb_{1-x}Te$ and $Ge_xSn_{1-x}Te$ alloys [12]. In case that as was explained referring to the higher low temperature electrical resistivity values, associated with lower carrier mobility values, compositional inhomogeneity is apparent for this low temperature hot pressing process, compositional variations in the investigated $(GeTe)_x(Bi_2Te_3)_{1-x}$ quasi-binary system, are expected to result is a decreased phase transition temperature from the low temperature rhombohedral to the high temperature cubic phases, with decreasing of the x values. As a result, a sequence of multiple $(GeTe)_x(Bi_2Te_3)_{1-x}$ compositions is expected to result in extended temperature range in which in the vicinity of each of the individual phase transition temperatures, associated with each of the apparent compositions, a continuous jump in both α and ρ values is expected. Such an effect can explain the abnormal trend observed in both α and ρ values following 450°C hot pressing. For the 650°C (~0.9 Tm) hot pressing temperature, the much more homogenized sate, associated with the much higher diffusion coefficients of each of the involved components, suppresses this effect dramatically.

Regarding the thermal conductivity values (Figure 5) obtained following the 650°C hot pressing conditions, lower

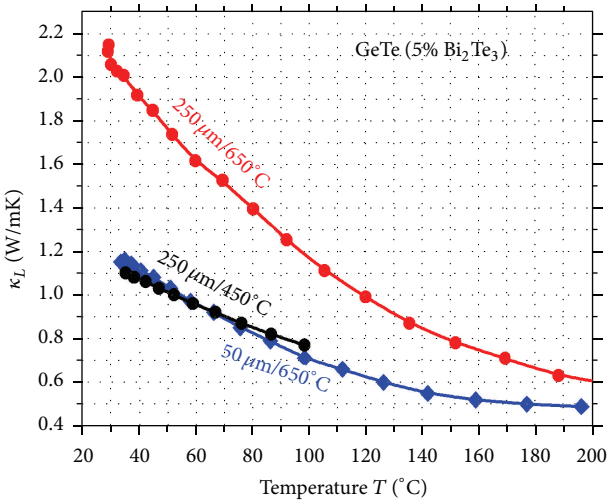

FIGURE 6: Temperature dependence of the lattice thermal conductivity, κ_L, for $(GeTe)_{0.95}(Bi_2Te_3)_{0.05}$ following hand crushing for maximal powder particles size of 50 and 250 μm and hot pressing at 650°C (50 μm/650°C and 250 μm/650°C, resp.) and for 250 μm hot pressed powder at 450°C (250 μm/450°C).

values were obtained following pressing of the maximal 50 μm powder agglomerates compared to the 250 μm condition. Some reduction of the thermal conductivity of the 50 μm powder is expected due to the slightly higher electrical resistivity values (Figure 4) and the consequently lower electronic thermal conductivity, κ_e, values, for this powder condition, as evidenced from the Wiedemann-Franz relation, $\kappa_e = (L/\rho)T$, where L and T are Lorenz number and absolute temperature, respectively. Yet, in order to explain the large (over than 20%) reduction of the thermal conductivity values of the "50 μm" compared to the "250 μm" sample, the lattice contribution to the thermal conductivity, κ_L, was also calculated for all of the investigated conditions as presented in Figure 6. For this calculation the reduced Fermi energy (η) was initially calculated at low temperatures (<200°C), for assuring an extrinsic region, using (1) and the measured Seebeck coefficient values (Figure 3) were taken into account:

$$\alpha = \frac{k}{e}\left[\frac{((5/2)+r)\,F_{(3/2)+r}}{((3/2)+r)\,F_{(1/2)+r}} - \eta\right], \quad (1)$$

where, e, k, F_r, η, and r are the electrons charge, Boltzmann constant, Fermi integral, the reduced Fermi energy (equals to $[E_F - E_V]/kT$ for p-type materials), and the scattering mechanism parameter (equal to −0.5 for the case of scattering by acoustic phonons as the dominant scattering mechanism, as is the case of GeTe), respectively.

Equation (1) is valid for a quadratic dependence of the carrier energy on the crystal momentum and a power dependence of the mean free time between electron collisions, τ on the kinetic energy ξ ($\tau = \tau_o \xi^r$, where τ_o is the constant), as for the case of GeTe based alloys. The heavy hole valence band, present in GeTe, was not taken into account, on account of its minor influence at low temperatures up to very high carrier concentrations of $\sim 7 \times 10^{26}$ m^{-3} [13].

At a second stage, the electronic contribution to the thermal conductivity, κ_e, was calculated using the Wiedemann-Franz relation described before, $\kappa_e = (L/\rho)T$, and the measured electrical resistivity values (Figure 4). Lorenz number, given by (2), was calculated using the reduced Fermi energy (η) values obtained from (1) at the initial stage of the calculation:

$$L = \left(\frac{k}{e}\right)^2 \left[\left(\left(r+\left(\frac{7}{2}\right)\right)\left(r+\left(\frac{3}{2}\right)\right) F_{r+(5/2)}(\eta)\, F_{r+(1/2)}(\eta) - \left(r+\left(\frac{5}{2}\right)\right)^2 F^2_{r+(3/2)}(\eta)\right) \times \left(\left(r+\left(\frac{3}{2}\right)\right)^2 F^2_{r+(1/2)}(\eta)\right)^{-1}\right]. \quad (2)$$

Finally, the lattice contribution to thermal conductivity, κ_L, was calculated by subtraction of κ_e from the measured total thermal conductivity, κ (Figure 5).

It can be clearly seen from Figure 6 that referring to the 650°C hot pressing condition, the "50 μm" sample exhibits much (reaching ~50%, at low temperatures) lower κ_L values compared to the "250 μm" sample. This result can be explained by the higher population of the less than 300 nm powder domains observed by the electronic microscopy (Figure 1) and XRD (Figure 2) analyses for the "50 μm" sample, in which higher mechanical stresses were applied during the ingot hand crushing procedures for passing the resultant powder, through the finer sieve size of 50 μm. The increased population of the <300 nm powder domains, which are considered as effective phonons scattering centers, is expected to result in lower κ_L values, observed in Figure 6.

Regarding the "250 μm" powder, much lower low temperature thermal conductivity values were obtained following the 450°C (compared to the 650°C) hot pressing condition, as can be also shown from Figure 5. Again, some reduction was expected due to the increased resistivity values for this sample (Figure 4) and the associated reduced κ_e values as was explained previously. However, further investigation of Figure 6 reveals that the lattice thermal conductivity values are also much lower for this sample, apparently due to the inhomogeneity associated with the lower diffusion rates of the involved matrix components and the possible presence of multiple closely related $(GeTe)_x(Bi_2Te_3)_{1-x}$ phases. The latter can also explain the abnormal temperature dependence of the thermal conductivity of this sample (Figure 5) which as was explained previously referring to the electrical resistivity trend (Figure 4) might be influenced by the appearance of a sequence of closely related $(GeTe)_x(Bi_2Te_3)_{1-x}$ phases, each associated with different individual phase transition temperature, leading to an extended temperature range of abnormal κ values.

The temperature dependence of the dimensionless figure of merit, ZT, following the various investigated experimental conditions is shown in Figure 7.

From this figure, it can be easily seen that for the homogenized samples obtained following 650°C hot pressing,

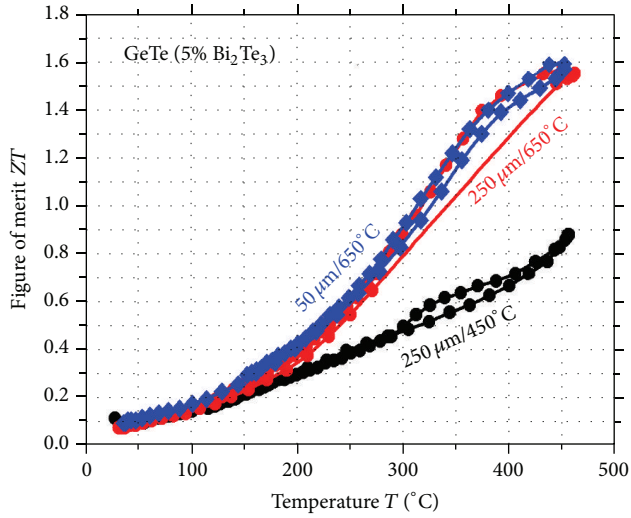

FIGURE 7: Temperature dependence of the dimensionless thermoelectric figure of merit, ZT, for $(GeTe)_{0.95}(Bi_2Te_3)_{0.05}$ following hand crushing for maximal powder particles size of 50 and 250 μm and hot pressing at 650°C (50 μm/650°C and 250 μm/650°C, resp.) and for 250 μm hot pressed powder at 450°C (250 μm/450°C).

much higher ZT values, compared to the nonhomogenized 450°C hot pressing condition, were obtained, exhibiting very high maximal values of ~1.6, which are among the highest so far reported for any p-type thermoelectric material. No practical differences were observed between the "50 μm" and "250 μm" conditions following 650°C hot pressing, probably due to a compensation of the slightly non-optimized carrier concentration, obtained for the "50 μm" powder due to the previously explained strain induced compensation effect, by the lower lattice conductivity values of this sample, which were associated with the higher population of low (<300 nm) dimensional powder domains.

4. Conclusions

In the current research the $(GeTe)_{0.95}(Bi_2Te_3)_{0.05}$ p-type thermoelectric composition was investigated following various processing routes for powdering and consolidation. High energetic ball milling at 700 RPM resulted in large XRD peaks broadening and even some amorphization. However hand crushing and sieving to a maximal 250 μm and 50 μm powder agglomerates resulted in crystalline powder particles, composed of much finer powder domains of less than 300 nm. The higher population of these powder domains resulted in lower lattice thermal conductivity for the 50 μm (compared to the 250 μm) powder. However, the higher strains associated with the increased mechanical force required for crushing the 50 μm powder into the desired size resulted in some reduction of the overall carrier concentration due to the strain induced compensation effect. Compensation of these two opposite effects resulted in similar very high maximal ZT values of up to 1.6 following consolidation, of both the 50 and 250 μm powder agglomerates, at 650°C, values which were found to be much higher than those obtained following the 450°C hot pressing condition. In the latter, a nonhomogenized matrix was attributed to lower diffusion rates of the involved components at this lower hot pressing temperature. The maximal ZT value of ~1.6 obtained following 650°C hot pressing is among the highest ever reported for any p-type thermoelectric material. Following the above conclusion, it seems possible to further enhance the obtained ZT values by annealing of the "50 μm" powder following the hand crushing procedure, for relieving the associated strains, prior the 650°C hot pressing procedure. Nevertheless, the annealing temperature should be carefully controlled for avoiding any undesired grain growth reactions. In this case, electronic transport properties similar to those obtained for the "250 μm" powder combined with the low κ_L values obtained for the "50 μm" powder, and consequently higher ZT values, are expected.

Conflict of Interests

The authors declare that there is no conflict of interests regarding the publication of this paper.

Acknowledgment

The work was partially supported by the EC FP7 *PowerDriver* Project.

References

[1] J. Sariel, I. Dahan, and Y. Gelbstein, "Rhombohedral-cubic phase transition characterization of (Pb,Ge)Te using high-temperature XRD," *Powder Diffraction*, vol. 23, no. 2, pp. 137–140, 2008.

[2] Y. Gelbstein, Y. Rosenberg, Y. Sadia, and M. P. Dariel, "Thermoelectric properties evolution of spark plasma sintered $(Ge_{0.6}Pb_{0.3}Sn_{0.1})Te$ following a spinodal decomposition," *Journal of Physical Chemistry C*, vol. 114, no. 30, pp. 13126–13131, 2010.

[3] Y. Gelbstein, B. Dado, O. Ben-Yehuda, Y. Sadia, Z. Dashevsky, and M. P. Dariel, "Highly efficient Ge-Rich Ge_xPb_{1-x} Te thermoelectric alloys," *Journal of Electronic Materials*, vol. 39, no. 9, pp. 2049–2052, 2010.

[4] Y. Gelbstein, B. Dado, O. Ben-Yehuda, Y. Sadia, Z. Dashevsky, and M. P. Dariel, "High thermoelectric figure of merit and nanostructuring in bulk p-type $Gex(Sn_yPb_{1-y})_{1-x}Te$ alloys following a spinodal decomposition reaction," *Chemistry of Materials*, vol. 22, no. 3, pp. 1054–1058, 2010.

[5] Y. Gelbstein, J. Davidow, S. N. Girard, D. Y. Chung, and M. Kanatzidis, "Controlling metallurgical phase separation reactions of the $Ge_{0.87}Pb_{0.13}Te$ alloy for high thermoelectric performance," *Advanced Energy Materials*, vol. 3, pp. 815–820, 2013.

[6] D. I. Bletskan, "Phase equilibrium in the system AIV-BVI—part II: systems germanium-chalcogen," *Journal of Ovonic Research*, vol. 1, no. 5, pp. 53–60, 2005.

[7] T. Caillat, M. Carle, D. Perrin, H. Scherrer, and S. Scherrer, "Study of the Bi-Sb-Te ternary phase diagram," *Journal of Physics and Chemistry of Solids*, vol. 53, no. 2, pp. 227–232, 1992.

[8] Y. Gelbstein, Z. Dashevsky, and M. P. Dariel, "High performance n-type PbTe-based materials for thermoelectric applications," *Physica B*, vol. 363, no. 1–4, pp. 196–205, 2005.

[9] Y. Gelbstein, Z. Dashevsky, and M. P. Dariel, "Powder metallurgical processing of functionally graded p-$Pb_{1-x}Sn_xTe$ materials for thermoelectric applications," *Physica B*, vol. 391, no. 2, pp. 256–265, 2007.

[10] Y. Gelbstein, Z. Dashevsky, and M. P. Dariel, "Highly efficient bismuth telluride doped p-type $Pb_{0.13}Ge_{0.87}Te$ for thermoelectric applications," *Physica Status Solidi*, vol. 1, no. 6, pp. 232–234, 2007.

[11] N. Bomshtein, G. Spiridonov, Z. Dashevsky, and Y. Gelbstien, "Thermoelectric, structural, and mechanical properties of spark-plasma-sintered submicro- and microstructured p-Type $Bi_{0.5}Sb_{1.5}Te_3$," *Journal of Electronic Materials*, vol. 41, no. 6, pp. 1546–1553, 2012.

[12] Y. Gelbstein, O. Ben-Yehuda, Z. Dashevsky, and M. P. Dariel, "Phase transitions of p-type (Pb,Sn,Ge)Te-based alloys for thermoelectric applications," *Journal of Crystal Growth*, vol. 311, no. 18, pp. 4289–4292, 2009.

[13] Y. Gelbstein, O. Ben-Yehuda, E. Pinhas et al., "Thermoelectric properties of (Pb,Sn,Ge)te-based alloys," *Journal of Electronic Materials*, vol. 38, no. 7, pp. 1478–1482, 2009.